Self-Assembly of A$\beta_{(10\text{-}35)}$-PEG Block Copolymer Fibrils

Timothy S. Burkoth,[†] Tammie L. S. Benzinger,[‡] Volker Urban,[§] David G. Lynn,*[,†] Stephen C. Meredith,*[,‡] and P. Thiyagarajan*[,§]

Departments of Chemistry and Pathology The University of Chicago, Chicago, Illinois 60637-1043 Intense Pulse Neutron Source, Argonne National Laboratory Argonne, Illinois 60439

Received April 19, 1999

β-sheet secondary structure is energetically dependent not only on the H-bonding interactions between individual strands, but also on the ability of the resulting sheet to twist, bulge, and fold into multifaceted macromolecular conformations.[1] Consequently, amino acid propensities have proven to be highly context-dependent, greatly complicating the design of peptides and proteins rich in β-structure.[2] Most problematic, however, are the intermolecular interactions which compromise solubility, the infamous feature of the many amyloid diseases.[3] We have exploited the energetics of self-association of amyloid peptides in the construction of a block copolymer consisting of the central domain from the β-amyloid peptide conjugated with poly(ethylene glycol) at the C-terminus, **1**.[4] The characteristics of **1** suggest a general strategy

1

for the construction of novel nanoscale materials of defined structure, ones in which the energetics of β-structural assembly may be exploited.

The existing models of the β-amyloid (Aβ) fibril predict that attachment of the PEG block to the hydrophobic domain would prevent fibril formation,[3,5] and yet **1** rapidly self-associates into fibrils, fibrils which remain soluble and whose degree of aggregation is mediated by simple modifications of concentration, pH, or ionic strength. The definition of the relative positions of the PEG and peptide blocks within the fibril becomes critical both to the further evaluation of the existing models of the Aβ fibril and to an understanding of the nature of the material. In this paper, using small angle neutron scattering (SANS) and electron microscopy (EM), we demonstrate the location and disposition of the PEG block to be on the surface of the fibril, ensuring the solubility of the fibrillar copolymer.

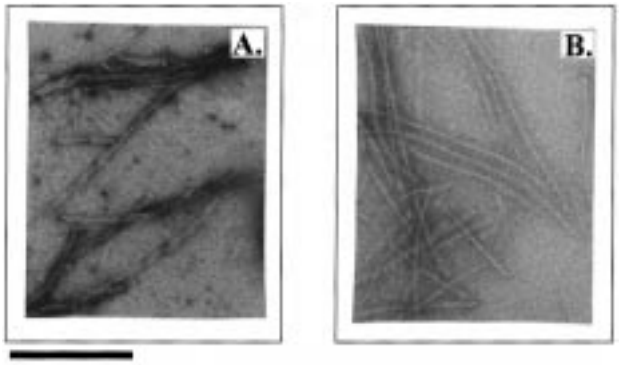

Figure 1. Electron micrographs of **1** titrated with A$\beta_{(10-35)}$ at pH 5.7. A: 100% A$\beta_{(10-35)}$ B: 1:1 A$\beta_{(10-35)}$:**1**. Black bar shows scale: 200 nm.

A polydisperse poly(ethylene glycol) block of 3 kDa was synthetically attached at the C-terminus of residues 10−35 of Aβ (A$\beta_{(10-35)}$) via solid-phase synthesis.[4] The purity of the peptide block of **1** was confirmed by CNBr cleavage product analysis.[4b] Circular dichroic spectra showed a reversible formation of β-strand structure as monitored by the single minima at $[\theta]_{217}$ and the fibrils bound by the dye Congo red, exhibiting the characteristic green-yellow birefringence.[4a] By EM,[6] **1** forms long, stable, individual fibrils with diameters >80 Å whose formation is readily reversed by changes in either pH or concentration.[4] In contrast, fibrils composed entirely of A$\beta_{(10-35)}$ did not form reversibly and contained bundles or twisted, paired fibrils, ∼90 by ∼160 Å with a superhelical repeat distance of ∼1100 Å and only occasional monomeric fibrils ∼80 Å diameter (Figure 1A). However, mixtures consisting of equal parts of **1** and A$\beta_{(10-35)}$ gave viscous solutions, and the lateral self-association and bundling of the fibrils was prevented (Figure 1B). This intermediate appearance is consistent with **1** and A$\beta_{(10-35)}$ forming mixed complexes, and the precise localization of the peptide and PEG blocks become critical to the understanding of the structure and physical characteristics of the material.

As seen in Figure 1, the A$\beta_{(10-35)}$ fibrils stain with a diffuse halo when mixed with **1**, a characteristic consistent with the PEG block localized to the surface of the fibril. To evaluate this localization directly, the radii in solution of both **1** and A$\beta_{(10-35)}$ fibrils were examined by SANS.[7] The intensity as a function of scattering angle for the samples[10] were interpreted with a modified Guinier analysis for rods which involves plotting $\ln[QI(Q)]$ versus Q^2.[11] Rodlike particles give rise to a linear region in the modified

* Authors for correspondence.
[†] Department of Chemistry, The University of Chicago.
[‡] Department of Pathology, The University of Chicago.
[§] Argonne National Laboratory.

(1) Salemme, F. R. *Prog. Biophys. Mol. Biol.* **1983**, *42*, 95−133. (b) Chothia, C. *Annu. Rev. Biochem.* **1984**, *53*, 537−572. (c) Rose, G. D.; Gierasch, L. M.; Smith, J. A. *Adv. Protein Chem.* **1985**, *37*, 1−109. (d) Nesloney, C. L.; Kelly, J. W. *Bioog. Med. Chem.* **1996**, *4*, 739−766.

(2) Minor, D. L., Jr.; Kim, P. S. *Nature* **1996**, *380*, 730−4. (b) Smith, C. K.; Regan, L. *Acc. Chem. Res.* **1997**, *30*, 153−61.

(3) Sipe, J. D. 1992 *Annu. Rev. Biochem.* **1992**, *61*, 947−975. Teplow, D. B. *Int. J. Exp. Clin. Invest.* **1998**, *5*, 121−142.

(4) Burkoth, T. S.; Benzinger, T. L. S.; Jones, D. N. M.; Hallenga, K.; Meredith, S. C.; Lynn, D. G. *J. Am. Chem. Soc.* **1998**, *120*, 7655−7656. (b) **1** was synthesized using standard fluorenyl-methoxy carbonyl protocols on PAP Tenta-Gel (Rapp Polymere). Cleavage by TFA and deprotection yielded a linear PEG 3000 covalently bound to the carboxyl terminus of the peptide. Peptide purity, determined by synthetic coupling yields and reverse phase HPLC of CNBr cleavage products, was >96%. Molecular masses of all peptides were verified by MALDI-TOF mass spectroscopy.

(5) Lansbury, P. T., Jr.; Costa, P. R.; Griffiths, J. M.; Simon, E. J.; Auger, M.; Halverson, K. J.; Kocisko, D. A.; Hendsch, Z. S.; Ashburn, T. T.; Spencer, R. G.; Tidor, B.; Griffin, R. G. *Nat. Struct. Biol.* **1995**, *2*, 990−998. Malinchik, S. B.; Inouye, H.; Szumowski, K. E.; Kirschner, D. A. *Biophys. J.* **1998**, *74*, 537−545. Lazo, N. D.; Downing, D. T. *Biochemistry* **1998**, *37*, 1731−1735.

(6) Samples of A$\beta_{(10-35)}$ and **1** were prepared for EM by diluting each dry peptide to 2 mM in water containing 0.1% NaN_3 (pH ≈ 3.0). The samples were mixed, centrifuged for 15 min at 14,000*g* and incubated for 1 h. The mixtures were then diluted to 1 mM in phosphate buffer at pH 5.7 and allowed to stand at room temp for 3 days. Samples were applied to a glow discharge 400 mesh carbon-coated support film, followed by staining with 1% uranyl acetate. Micrographs were recorded using Philips EM 300 at magnifications of 100,000, 45,000, and 10,000.

(7) SANS experiments were performed by SAND at the Intense Pulsed Neutron Source of Argonne National Laboratory.[8] Pulsed neutrons, $\lambda = 0.5-14$ Å, were detected with a 128 × 128 array of position-sensitive gas-filled 40 × 40 cm^2 proportional counters, and the wavelengths were measured with time-of-flight by binning the pulse to 68 constant $\Delta\lambda/\lambda = 0.05$ time channels. This instrument provides a useful range of momentum transfer ($Q = 4\pi \sin(\theta)/\lambda$, where θ is half the scattering angle and λ is the wavelength of the probing neutrons) of 0.0035−0.6 $Å^{-1}$ in a single measurement. The measurements on the samples in 16% D_2O were made on SAD[9] which is similar to SAND, but the Q range is limited to 0.005−0.25 $Å^{-1}$.

(8) Thiyagarajan, P.; Urban, V.; Littrell, K.; Ku, C.; Wozniak, D. G.; Belch, H.; Vitt, R.; Toeller, J.; Leach, D.; Haumann, J. R.; Ostrowski, G. E.; Donley, L. I.; Hammonds, J.; Carpenter, J. M.; Crawford, R. K. Proceedings 14th Meeting of the International Collaboration on Advanced Neutron Sources, June 14−19, 1998, Utica, IL 864−878.

(9) Thiyagarajan, P.; Epperson, J. E.; Crawford, R. K.; Carpenter, J. M.; Klippert, T. E.; Wozniak, D. G. *J. Appl. Crystallogr.* **1997**, *30*, 280−293.

10.1021/ja991233x CCC: $18.00
Published on Web 07/27/1999

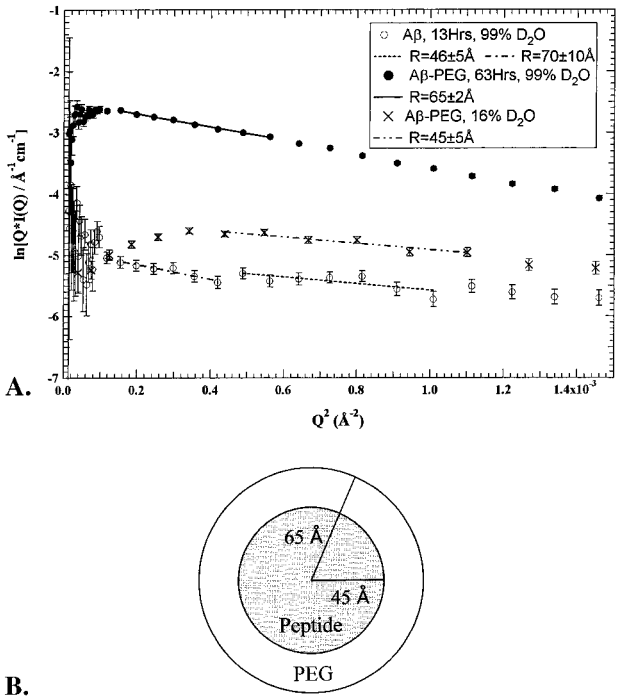

Figure 2. SANS data fit to a modified Guinier plot for a rod-like form of A$\beta_{(10-35)}$ (○) and **1** (●) in 99% D_2O buffer. The average radii were calculated to be 46 (±5) Å and 65 (±2) Å, respectively. **1** in 16% D_2O (×) to match the coherent scattering from PEG gave a radius of 45 ± 5 Å. Below a schematic representation of peptide and PEG blocks in the fibril.

Guinier plot in the low Q region ($Q_{max}R_c = 1.0$) where the cross sectional radius of gyration of the rod R_c can be derived from the slope of the straight line by $R_c^2 = -2 \times$ slope.[12] The radius of the rod is $R = \sqrt{2}R_c$. Figure 2 shows that the average radius of A$\beta_{(10-35)}$ in 99% D_2O buffer at pH 5.6 was 46 ± 5 Å. In addition, the slightly larger slope in the low Q region is consistent with the presence of rods of a larger radius, 70 ± 10 Å, similar to the fibril−fibril association observed by EM in Figure 1A. The SANS data for the fibrils of **1** under the same conditions showed no evidence of fiber−fiber association, but detected a single species with a radius of 65 ± 2 Å. Thus, the PEG moiety increases the radius of the fiber by about 20 ± 5 Å.

Contrast matching via adjustment of the deuteration level of the solvent eliminated the scattering due to PEG and thus selectively measured the peptide portion of the fibril.[13] In 16% D_2O, the contrast factor to render PEG invisible, the fibrils formed with **1** had a radius of 45 ± 5 Å. This dramatic change in radii between the Aβ-PEG samples in 16 and 99% D_2O confirms the conclusions from EM analyses that the PEG block is localized at the periphery of the fibrils. Most importantly, the macromolecular organization of the peptide portion of both fibrils appears identical. In this context, solid-state NMR experiments on A$\beta_{(10-35)}$ fibrils had established that an extended parallel β-sheet was oriented perpendicular to the fiber axis to give an extended β-helix conformation,[14] a structure proposed to be a common feature of all amyloids.[15]

Aβ-PEG positions the PEG block along the surface of the fibril, and its localization at the hydrophobic C-terminus is sufficient to retard fibril−fibril contact and precipitation.[4a] By implication, A$\beta_{(10-35)}$ positions the hydrophobic C-terminus of the peptide on the fibril surface, but this arrangement is inconsistent with the current Aβ models which bury the hydrophobic residues within the fibril. Although A$\beta_{(10-35)}$ and A$\beta_{(1-42)}$ may self-assemble differently, A$\beta_{(10-35)}$ fibrils are morphologically similar to those of the full-length peptide, and unlike more extensive C-terminal truncations, A$\beta_{(10-35)}$ retains the ability to add to bona fide Alzheimer's plaques.[16] Furthermore, both A$\beta_{(10-35)}$ and A$\beta_{(1-42)}$ fibrils undergo identical side chain−side chain cross-linking reactions,[4a,14,17] suggesting that there are significant structural similarities between the fibrils.

More generally, we have exploited the association energies of amyloid peptides and constructed a block copolymer whose self-assembly is both dominated by the peptide and formed under thermodynamic control. The peptide core of the fibril is paracrystalline[18] and consists of laminated parallel β-sheets with each amino acid in register along an extended β-helix.[14] This fibrillar structural scaffold therefore has a peptide core of defined secondary structure and can now be easily manipulated with synthetic modification to both blocks. Recently, others have also reported on the formation of tubular micelle-like aggregates from structurally divergent block copolymers.[19] The synthetic flexibility offered by this material will allow for the engineering of tertiary structure and large functional macromolecules whose macromolecular self-assembly can be readily controlled.

Acknowledgment. We thank ANL and the NIH (R21 RR 12723, D.G.L.) for support and the NIH (5 T32 HL07327, T.S.B.; 5 T32 GM07281, T.L.S.B.), for fellowships. This work benefited from the use of facilities in the IPNS, which is funded by the U.S. DOE, BES under contract W-31-109-ENG-38 to the University of Chicago.

JA991233X

(10) A$\beta_{(10-35)}$ (5.77 mg/mL) and **1** (11.5 mg/mL) in 99% D_2O buffer at pH = 5.6 were analyzed in 5-mm quartz cells, and **1** (11.5 mg/mL) in 16% D_2O buffer at pH = 5.7 was analyzed in 1-mm quartz cells. The evolution of the scattering signal from the samples in 99% D_2O was followed for several hours at 22 °C, with each measurement lasting for 1 h, to ensure that the samples had reached thermodynamic equilibrium at the length-scales being measured. Each of the samples in 16% D_2O was measured using SAD for about 20 h. The scattering data were corrected for the background from the instrument; the sample cell, and the solvent and the data were further normalized for the concentration of sample in mg/cm^3. The differential scattering cross-section, $I(Q)$, in the absence of interparticle correlation, is given by $I(Q) = N_p \cdot V_p 2(\rho_p - \rho_r)^2 F(Q)$ where N_p is the number of particles in unit volume, V_p is the volume of the particles, $F(Q)$ is the form factor describing the shape of the particles, and ρ_p and ρ_r are the neutron scattering length densities of the particle and the solvent, respectively. The scattering length density ρ for any system can be calculated by using

$$\rho = N_A d \left[\sum_i b_i / \sum_i M_i\right]$$

where b_i and M_i are the neutron scattering length and mass of ith atoms in the system respectively, d is the density of the system, and N_A is Avogadro's number.

(11) Thiyagarajan, P.; Chaiko, D. J.; Hjelm, R. P., Jr. *Macromolecules* **1995**, *28*, 7730−7736.

(12) Porod, G. In *Small Angle X-ray Scattering*; Glatter, O., Kratky, O., Eds.; Academic Press: New York, 1982; Chapter 2.

(13) The difference in the scattering length densities of the particle and the matrix is known as the contrast. $I(Q)$ will be zero if the scattering length density of the particle is equal to that of the solvent. Since the scattering length density values of H_2O, D_2O, PEG, and the peptide are -0.56×10^{10} cm^{-2}, 6.34×10^{10} cm^{-2}, 0.57×10^{10} cm^{-2}, and 1.93×10^{10} cm^{-2}, respectively, the coherent scattering from PEG can be eliminated if 16% D_2O buffer is used.[9]

(14) Benzinger, T. L. S.; Gregory, D. M.; Burkoth, T. S.; Miller-Auer, H.; Lynn, D. G.; Botto, R. E.; Meredith, S. C. *Proc. Natl. Acad. Sci. U.S.A.* **1998**, *95*, 13407−13412. Burkoth, T. S.; Benzinger, T. L. S.; Urban, V.; Gregory, D. M.; Thiyagarajan, P.; Botto, R. E.; Meredith, S. C.; Lynn, D. G., submitted.

(15) Blake, C.; Serpell, L. *Structure* **1996**, *4*, 989−998.

(16) Esler, W. P.; Stimson, E. R.; Ghilardi, J. R.; Vinters, H. V.; Lee, J. P.; Mantyh, P. W.; Maggio, J. E. *Biochemistry* **1996**, *35*, 749−747. Esler, W. P.; Stimson, E. R.; Ghilardi, J. R.; Lu, Y.-A.; Felix, A. M.; Vinters, H. V.; Mantyh, P. W.; Lee, J. P.; Maggio, J. E. *Biochemistry* **1996**, *35*, 13914−21.

(17) Selkoe, D. J.; Abraham, C.; Ihara, Y. *Proc. Natl. Acad. Sci. U.S.A.* **1982**, *79*, 6070−6074. Ikura, K.; Takahata, K.; Sasaki, R. *FEBS Lett.* **326**, 109−111.

(18) The term *paracrystalline* refers to highly ordered supramolecular aggregates, which do not, however, attain long range order in all three dimensions.

(19) Yu, Y.; Zhang, L.; Eisenberg, A. *Macromolecules* **1998**, *31*, 1144−54. Yamada, N.; Ariga, K.; Naito, M.; Matsubara, K.; Koyama, E. *J. Am. Chem. Soc.* **120**, 12192−99. Won, Y.-Y.; Davis, H. T.; Bates, F. S. *Science* **1999**, *283*, 960−3.